Received: 25 January 2021 | Accepted: 29 January 2021

DOI: 10.1002/prp2.737

ORIGINAL ARTICLE

ZINC40099027 activates human focal adhesion kinase by accelerating the enzymatic activity of the FAK kinase domain

Rashmi[1] | Shyam K. More[1] | Qinggang Wang[1] | Emilie E. Vomhof-DeKrey[1,2] | James E. Porter[2] | Marc D. Basson[1,2,3]

[1]Department of Surgery, University of North Dakota School of Medicine & Health Sciences, Grand Forks, ND, USA

[2]Department of Biomedical Sciences, University of North Dakota School of Medicine & Health Sciences, Grand Forks, ND, USA

[3]Department of Pathology, University of North Dakota School of Medicine & Health Sciences, Grand Forks, ND, USA

Correspondence
Marc D. Basson, Department of Surgery, University of North, Dakota School of Medicine and Health Sciences, 1301 North Columbia Road, Grand Forks, ND 58202, USA.
Email: marc.basson@und.edu

Funding information
National Institute of General Medical Sciences, Grant/Award Number: UT2GM130175; National Institute of General Medicine, Grant/Award Number: UT2GM130175; National Institutes of Health

Abstract

Focal adhesion kinase (FAK) regulates gastrointestinal epithelial restitution and healing. ZINC40099027 (Zn27) activates cellular FAK and promotes intestinal epithelial wound closure in vitro and in mice. However, whether Zn27 activates FAK directly or indirectly remains unknown. We evaluated Zn27 potential modulation of the key phosphatases, PTP-PEST, PTP1B, and SHP2, that inactivate FAK, and performed in vitro kinase assays with purified FAK to assess direct Zn27-FAK interaction. In human Caco-2 cells, Zn27-stimulated FAK-Tyr-397 phosphorylation despite PTP-PEST inhibition and did not affect PTP1B-FAK interaction or SHP2 activity. Conversely, in vitro kinase assays demonstrated that Zn27 directly activates both full-length 125 kDa FAK and its 35 kDa kinase domain. The ATP-competitive FAK inhibitor PF573228 reduced basal and ZN27-stimulated FAK phosphorylation in Caco-2 cells, but Zn27 increased FAK phosphorylation even in cells treated with PF573228. Increasing PF573228 concentrations completely prevented activation of 35 kDa FAK in vitro by a normally effective Zn27 concentration. Conversely, increasing Zn27 concentrations dose-dependently activated kinase activity and overcame PF573228 inhibition of FAK, suggesting the direct interactions of Zn27 with FAK may be competitive. Zn27 increased the maximal activity (V_{max}) of FAK. The apparent K_m of the substrate also increased under laboratory conditions less relevant to intracellular ATP concentrations. These results suggest that Zn27 is highly potent and enhances FAK activity via allosteric interaction with the FAK kinase domain to increase the V_{max} of FAK for ATP. Understanding Zn27 enhancement of FAK activity will be important to redesign and develop a clinical drug that can promote mucosal wound healing.

KEYWORDS
focal adhesion kinase, migration, mucosal repair, nonsteroidal anti-inflammatory drugs

Abbreviations: EC_{50}, effective concentration of drug that gives 50% of maximal response; FAK, Focal Adhesion Kinase; IBD, Inflammatory Bowel Disease; KD, Kinase Domain; NSAIDs, Nonsteroidal anti-inflammatory drugs; PF573228, 6-[[4-[(3-methylsulfonylphenyl) methylamino]-5-(trifluoromethyl) pyrimidin-2-yl] amino]-3,4-dihydro-1H-quinolin-2-one; PTP LYP inhibitor, (2-pyridine) $(Ph)_2$P-Au-Cl; PTP1B, Protein tyrosine phosphatase 1B; PTP-PEST, Protein tyrosine phosphatase enriched with proline, glutamic/aspartic acid and serine/threonine residues; SHP2, SRC Homology 2 domain-containing phosphatase 2; ZINC40099021, 2-(3-methoxyphenyl)-N-[2-(morpholin-4-yl)-5-(trifluoromethyl) phenyl] pyrrolidine-1-carboxamide; ZINC40099027, 2-(4-methoxyphenyl)-N-(2-morpholino-5-(trifluoromethyl) phenyl) pyrrolidine-1-carboxamide.

1 | INTRODUCTION

Mucosal healing is an important treatment goal for a wide range of gastrointestinal disorders including peptic ulcers, inflammatory bowel disease, and injury from nonsteroidal anti-inflammatory drugs.[1] Whether the mucosa heals depends upon the balance between ongoing injury and mucosal repair mechanisms.[2] Therapy is generally directed at reducing or blocking the injurious stimulus. Depending upon the disease, such treatment may include blocking acid secretion, eradicating *Helicobacter pylori* (*H. pylori*), or reducing inflammation with general immunosuppressive agents or antibodies that target specific inflammatory cytokines. Although a broad range of treatment strategies focus on ameliorating ongoing injury, no therapeutic agents are available to directly stimulate mucosal healing itself.

Mucosal wound healing is a complex process, but epithelial sheet migration across the mucosal defect is critical to healing.[3,4] Epithelial cell migration plays a crucial role in several metabolic pathways,[5] and is regulated by a web of intracellular signals[6] as well as interaction with other cell types,[7,8] and luminal nutrients.[9,10] During cell adhesion and migration, assembly, and disassembly of matrix cell adhesion sites take place.[11]

FAK is a 125 kDa multidomain protein ubiquitously expressed as a nonreceptor cytoplasmic protein tyrosine kinase.[12] FAK localized at focal adhesions is a key mediator of integrin and growth factor-mediated signaling.[13] FAK influences cell adhesion, migration, and proliferation by mediating the cell's responses to adhesion-dependent signaling or lack thereof[14] and the response to physical forces like repetitive deformation.[15–17] Although FAK is critical to epithelial sheet migration, its activity is decreased in migrating gut epithelial cells at the edge of defects in vitro[18] and in vivo,[19] making it an attractive target for therapy to remediate this defect and thus promote mucosal healing.

Previously, we serendipitously identified two novel small molecules that may mimic the four-point-one, ezrin, radixin, moesin (FERM) domain of FAK in intestinal epithelial cancer cell lines at concentrations as low as 10 nM.[20] We have previously reported that Zn27 activates FAK and stimulates intestinal epithelial migration in vitro and mucosal healing in vivo. Although we did not do a full dose–response range study in our previous report, Zn27 effectively stimulated FAK phosphorylation in human Caco-2 intestinal epithelial cells by approximately 18% at concentrations as low as 10 nM, whereas a greater 36% effect was observed at 1000 nM. Similarly, the closure of wounds in Caco-2 monolayers was accelerated by 20% at 10 nM and 63% at 100 μM of Zn27. In vivo, we studied only a single dose level of 900 μg/kg, administered every 6 h intraperitoneally. After a single administration, this dose led to peak levels of 22.25 at 1 h and trough levels of 4 nM by 6 h. Repeated dosing over 3 days allowed some accumulation such that we observed a final trough level of 4.6 nM, just below the lowest level at which we had observed in vitro efficacy. This dosing range produced substantial effects in vivo. Mucosal healing of circumscribed small intestinal ischemic ulcers was accelerated approximately 3.5-fold by Zn27 versus healing rates in vehicle-treated control mice. In a separate indomethacin-induced model of multiple small bowel ulceration, total small bowel ulcer area in mice receiving Zn27 was approximately half that in vehicle-treated control mice, whereas increased phosphor-FAK immunoreactivity was observed in the mucosa adjacent to these ulcers. Pyk2 is the kinase closest to FAK in structure, whereas Src is a second prototypical nonreceptor tyrosine kinase in the focal adhesion complex. Neither was activated by Zn27 in Caco-2 cells even at a concentration of 1000 nM, 100-fold higher than the concentration required to activate FAK, suggesting the potential specificity of this molecule for FAK activation.[21]

It, therefore, became important to understand how treating cells or mice with this molecule results in increased FAK activity. Since Zn27 treatment increases FAK phosphorylation at Tyr-397, which is generally held to be a FAK autophosphorylation site,[21,22] it seemed less likely that the molecule activates FAK by activating some other kinase that would then secondarily activate FAK. Competing hypotheses, therefore, included the possibility that Zn27 interferes with one of the tyrosine phosphatases that inactivates FAK or that Zn27 activates FAK directly. We now, therefore, sought to distinguish among these possibilities and determine the mechanism by which Zn27 activates FAK to promote wound closure.

Significance statement

Focal adhesion kinase is an attractive target to promote gastrointestinal mucosal healing. Zn27 activates FAK to heal murine intestinal ulcers, but its mechanism remains unclear. This study demonstrates that Zn27 is a potent, selective, and direct activator of the FAK kinase domain. Zn27 allosterically interacts directly with FAK to increase its V_{max}. Understanding the characteristics and mechanism of this prototypical enhancer of FAK activity will facilitate the design of clinically useful therapeutics to promote mucosal wound healing.

2 | MATERIALS AND METHODS

2.1 | Chemicals and reagents

Dulbecco's modified Eagle's medium and Trypsin EDTA were from Thermo Fisher. The following primary antibodies were used for immunoprecipitation or western blot analysis: FAK-Tyr-397 (1:1000, ab81298; Abcam; total FAK (1:2000, Anti-FAK, clone 4.47, 05-537; 1: EMD Millipore); GST 26H1 (1:1000, mouse mAb, 2624); His-Tag 27E8 (1:1000, Mouse mAb, 2366); and Anti-PTP1B (1: 1000, 5311S) were from Cell Signaling. Mouse IgG (1:200, SC-2025) was from Santa Cruz Biotechnology, Inc. Protein G plus/protein A agarose suspension beads IP05-1.5 ml were from Merck, Millipore.

The infrared fluorescence dye (IRDye) detection method was used to visualize the immunoblots. IRDye conjugated secondary antibodies were rabbit IRDye 680/800 (P/N 925-68073/P/N 925-32213) and mouse IRDye 680/800 (P/N 925-68072/P/N 925-32212). Secondary antibodies anti-rabbit 680/800 and anti-mouse 680/800 were from LI-COR. Secondary antibody IgG (Mouse monoclonal [SB62a] Anti-Rabbit IgG light chain (HRP), 1:10000, ab99697, Abcam). The homogeneous full-length SHP-2 activity assay kit (79330) was from BPS Bioscience.

2.2 | Activators and inhibitors

ZINC40099027 (Zn27; Z410149492), and ZINC40099021 (Zn21; Z410148286) were supplied by Enamine (Monmouth Jct.). For studies of tyrosine phosphatase activity, PTP-PEST was inhibited using PTP LYP inhibitor (540217; Calbiochem-Millipore Sigma). The FAK inhibitor PF573228 was from Selleck Chemicals. The stocks for drugs were prepared in 100% DMSO solution, then diluted into a culture medium for cell-based experiments and into distilled water for in vitro kinase studies. Final DMSO concentration in cell-based studies did not exceed 0.05% and did not exceed 0.005% for the in vitro kinase assays.

2.3 | Cell culture

Caco-2 cells were obtained from the ATCC and cultured as previously described.[23] As the signal cascade examined herein occurs in suspended cells before adhesion, 80%–90% confluent Caco-2 cells were seeded into cell culture dishes precoated with 1% heat-inactivated bovine serum albumin (BSA, Sigma-Aldrich, Merck) to prevent adhesion as previously described.[24] Caco-2 cells were pretreated with 50 μM PTP LYP inhibitor or 10 nM Zn27 and incubated for 1 h at 37°C and 8% CO_2. For studies to evaluate the effect of FAK inhibition on the effects of Zn27, Caco-2 cells were seeded in BSA-coated plates and incubated with 10 μM PF573228 in the presence or absence of 10 nM Zn27 for 1 h.

2.4 | Western blotting

Cell lysates were prepared using lysis buffer (50 mM Tris, 150 mM NaCl, 1 mM EDTA, 1 mM EGTA, 1% TritonX100, 1% deoxycholic acid, 0.1% SDS, 10% glycerol, and protease and phosphatase inhibitors). The concentration of protein in the lysate was estimated using the bicinchoninic acid (BCA) assay technique (Pierce). For cell-based studies, sample preparation was done in 6X Laemmli buffer (Alfa Aesar, J61337-AD, Thermo Fisher Scientific). The samples were then resolved by 10% SDS-PAGE, transferred onto nitrocellulose membranes, blocked with Odyssey TBS Blocking Buffer (Amersham Life Science), and incubated at 4˚C overnight with primary antibodies for FAK-Tyr-397 or FAK. Secondary antibodies were used at 1:10,000 dilution and incubated at room temperature for 1 h. Membranes were visualized by the IRdye fluorescent system using an Odyssey Fc Imaging System (LI-COR Biosciences). Images were captured and analyzed using LI-COR software Image Studio Lite v.5.x (LI-COR Biosciences).

Separate Western blots were performed to determine the effect of 10 nM Zn27 on purified 125 kDa and 35 kDa FAK. Sample preparation for this in vitro kinase assay was carried out in 20 μl of reaction volume.[25] The reaction mixtures contained 300 μM ATP, 2X Kinase reaction buffer C (2X KRBC) (1 mM DTT, 2.5 mM MnCl2, 5X kinase reaction buffer A), 1 μl DMSO or Zn27, and 100 ng of 125kda or 35kda FAK (Signal Chem). The reaction mixtures were incubated for 30 min at room temperature before Western blot analysis. Membranes were probed with primary antibodies for FAK-Tyr-397, GST, and His-Tag. The secondary antibodies were used at 1:10,000 and incubated at room temperature for 1 h. The membranes were visualized as described above.

2.5 | Co-immunoprecipitation studies

Suspended Caco-2 cells were treated with vehicle control DMSO and/or 10 nM Zn27 in dishes precoated with 1% heat-inactivated BSA at 37°C in 8% CO_2. After a 1 h incubation, cells were lysed in a nondenaturing lysis buffer (Pierce IP Lysis Buffer, Cat. No. 87788, Thermo Fisher Scientific Inc) and a 1–2 mg of protein was used for each immunoprecipitation. For immunoprecipitation of FAK, the total protein was incubated with mouse anti-FAK antibody, at 4°C overnight. Normal mouse IgG was used as a control antibody for the co-immunoprecipitation. Protein G plus/protein A agarose suspension beads were added to the lysate containing anti-FAK and incubated for an extra 2 h at 4°C. Then, the beads were washed, and protein was eluted in 6X Laemmli buffer (Alfa Aesar, J61337-AD, Thermo Fisher Scientific). The eluted protein samples were resolved by 10% SDS-PAGE, transferred to a nitrocellulose membrane, and immunoblotted with the anti-FAK antibody for IP. The immunoprecipitated blots were then probed with anti-PTP1B to assess co-precipitating PTP1B associated with FAK. The secondary antibody anti-mouse 800 was used for detection of FAK and the detection of PTP1B, anti-secondary Ab mouse monoclonal secondary antibody to Rabbit IgG light chain (HRP) was used. The total lysates loaded on gel and western blotted served as input control for the Co-IP. The images were acquired by LICOR imaging for FAK, whereas the chemiluminescence detection system and Biorad gel doc were used for PTP1B. Densitometric quantitation was performed with LICOR imaging (LI-COR Biosciences).

2.6 | Phosphatase (SHP2) activity assay

The SHP-2 activity assay is a two-step protocol using the homogeneous full-length SHP-2 assay kit (79330) from BPS Bioscience. In the first step, SHP2 is activated in the presence of peptide. In the second step, the fluorogenic substrate DiFMuP is added to release DiFMu fluorophore. The assay was performed in a total reaction volume of 25 μl at room temperature for 30 min in a 96 well, black, low-binding microtiter plate (Corning, 3631). The 25 μl reaction

mixture consisted of 5X assay buffer, SHP2 activating peptide (5 μM), DTT (5 mM), SHP2 enzyme (0.2 ng/μl), 10 nM Zn27. SHP2 activation was monitored using SHP2 substrate (DiFMUP) 25 μl per well. Fluorescence intensity was measured using a microplate reader (Biotek) using Ex/Em=360 ± 20/460 ± 20 nm reader.

2.7 | In vitro kinase assay

Highly purified recombinant full-length 125 kDa (1–1157aa) and 35 kDa (393–698aa) human FAK expressed with baculovirus in Sf9 insect cells using an N-terminal GST tag (No. P91-10G) for 125 kDa an N-terminal His tag (P91-11H) for 35 kDa were obtained from Signal Chem. The FAK Kinase Enzyme System (V9301, Promega) was used for in vitro kinase enzymatic assay. The effect of Zn27 (Enamine, Monmouth Jct.) on FAK activity was measured using a luminescent assay. Luminescence was measured using a Tecan Spark plate reader (Tecan Spark®, Tecan Trading AG). Concentration-dependent studies were performed using 0 to 100 nM Zn27. Iterative nonlinear regression analysis was used to calculate the EC_{50} concentration of Zn27 that generated half-maximal amounts of FAK activity.[26]

2.8 | Competition studies of Zn27 in presence of a FAK inhibitor

The FAK inhibitor PF573228 (0–1000 μM) was tested for its interactions with the effect of Zn27 on the activity of the 35 kDa FAK kinase domain. The reaction mixture (25 μl/well) included 5 μl ATP (30 μM), 2X KRBC (5X kinase reaction buffer A, 1 mM DTT, 2.5 mM MnCl2), FAK (12.5 ng/μl), and Zn27 (0–100 nM). Zn21 (10 nM) was used as a negative control. After a 30-min incubation, 5 μl of 10 mM polypeptide substrate (4:1 Glu; Tyr) was added to each well for 60 min. ADP-Glo (25 μl) was then added to each well to deplete ATP, leaving only ADP and very low background of ATP, and thus stopping the reaction. After 40 min further incubation, 50 μl of kinase detection reagent was added to each well to convert the new ADP back to ATP, and luciferase and luciferin were introduced for detection of ATP followed by a 30-min incubation at 25°C. Luminescence intensity was measured using the Tecan Spark plate reader (Tecan Spark®, Tecan Trading AG). The enzyme activity was calculated by first subtracting the signal obtained from the negative control (no enzyme and no drug). The kinase activity signal without drug was used as a positive control and the effects of increasing concentrations of Zn27 were assessed as fold change over the kinase activity signal without Zn27.

2.9 | Michaelis–Menten saturation kinetics assay

Saturation kinetic studies were performed using the in vitro kinase assay with increasing concentrations of ATP (0–300 μM), with and without FAK, in the presence or absence of 10 nM Zn27 at room temperature for 30 min. Total luminescence (FAK +Zn27 or control) and nonspecific luminescence (no FAK +Zn27 or control) were measured at each ATP concentration. Specific luminescence was calculated as the difference between total luminescence and nonspecific luminescence.[10] From the plotted saturation hyperbola, maximal velocity of FAK enzymatic activity (V_{max}) and equilibrium dissociation constant (K_m) of ATP for the kinase was calculated using iterative nonlinear regression analysis.[26]

2.10 | Statistical analysis

All statistical analyses were performed using GraphPad Prism software version 9). All the results were expressed as mean ± standard error. In all experiments, q test was applied to remove outliers. Statistical analysis was performed using t-test for normally distributed data, seeking 95% confidence. For comparing more than two sets of data, ordinary one-way ANOVA was performed using *post hoc* Tukey's multiple comparison test for PTPLYP inhibitor study and *post hoc* Sidak's multiple comparisons test[27] for studies of PF573228 with or without Zn27. All iterative nonlinear regression analysis was performed using GraphPad Prism software (version 9). A *p*-value of less than .05 was considered statistically significant. *n* equals the number of individual experiments.

For complex experiments with small experimental effect sizes, we performed initial sample calculations to determine the number of studies to be performed. This was done by G* Power 3.[28] In some instances, we first did 6–8 experiments to help estimate the initial information required for the sample size calculation, including the mean value to be observed under baseline control conditions and the expected standard deviation of our experimental results.

The competition displacement study analyzing the effects of the FAK inhibitor PF573228 on the effects of Zn27 was performed for varying concentrations of Zn27 (0.01, 0.1, 1, 10, 100 nM) in the presence or absence of PF573228 (10 nM). A multiple nonparametric Mann–Whitney t-test was performed to show that values for Zn27 and Zn27+PF573228 were statistically different at each concentration of Zn27. A curve fitting nonlinear regression analysis for variable slope was performed to assess the competitive property of Zn27 in the presence or absence of PF573228 for each experiment. The function used to calculate the EC_{50} was "log dose versus response-variable slope (four parameters)." The Hill slope equation is based on the following equation: $Y = \text{Bottom} + (\text{Top}-\text{Bottom})/(1 + 10^{((\text{LogEC50-X}) \times \text{Hill Slope})})$. The EC_{50}'s calculated for each experiment for Zn27 alone were then statistically compared with the EC_{50}'s calculated for Zn27 in the presence of PF573228 by an unpaired t-test, seeking 95% confidence.

2.11 | Nomenclature of targets and ligands

Key protein targets and ligands in this article are hyperlinked to corresponding entries in http://www.guidetopharmacology.org, the common portal for data from the IUPHAR/BPS Guide to

PHARMACOLOGY,[29] and are permanently archived in the Concise Guide to PHARMACOLOGY 2019/20 (Alexander et al., 2019).

3 | RESULTS

3.1 | Zn27 does not modulate FAK by regulating the tyrosine phosphatases that are known to inactivate FAK

The cytosolic phosphatases SHP2 (SRC Homology 2 domain-containing phosphatase 2; 30), PTP-PEST (Protein tyrosine phosphatase enriched with proline, glutamic/aspartic acid, and serine/threonine residues,[31,] as well[32] as the membrane-bound phosphatase PTP1B (Protein tyrosine phosphatase 1B; 33) are all known to dephosphorylate FAK at Tyr-397. We evaluated the possibility that Zn27 might interact with one of these three tyrosine phosphatases to indirectly cause FAK activation. We first assessed the ability of PTP-PEST inhibition to block induction of FAK-Tyr-397 autophosphorylation by Zn27. We treated human Caco-2 intestinal epithelial cells with 50 μM of the PTP-PEST inhibitor, PTP LYP in the absence or presence of 10 nM Zn27. The concentration of PTP LYP inhibitor used far exceeded its IC_{50} of 1.5 μM,[34] essentially blocking PTP-PEST phosphatase activity. The concentration of Zn27 used was based on our previous study which demonstrated that Zn27 treatment resulted in increased FAK-Tyr-397 phosphorylation and epithelial wound healing both in vitro and in vivo at approximately this concentration.[21] Although PTP-PEST inhibition dramatically enhanced FAK phosphorylation, Zn27 stimulated FAK phosphorylation similarly in either the absence or presence of PTP LYP (15.4 ± 6% vs. 15 ± 20%, respectively, Figure 1A and B, $n = 25$, $p < .05$).

We next investigated whether Zn27 modulates FAK-PTP1B interaction. Treatment with Zn27 did not change FAK-PTP1B interaction, making it unlikely that Zn27 activates FAK by modulating PTP1B (Figure 1C and D). Finally, we measured the activity of SHP2 in the absence or presence of 100 nM Zn27 and found no differences in the amount of dephosphorylated fluorogenic substrate with Zn27 than without it (Figure 1E). Taken together, these results did not suggest that Zn27 activates FAK by inhibiting one of these key tyrosine phosphatases.

3.2 | Zn27 is a potent activator of FAK

Since, it seemed less likely that Zn27 modulates FAK indirectly by affecting tyrosine dephosphorylation, we next investigated the possibility that Zn27 directly activates FAK. We studied both purified N-terminal GST-tagged full-length FAK (125 kDa) and the N-terminal

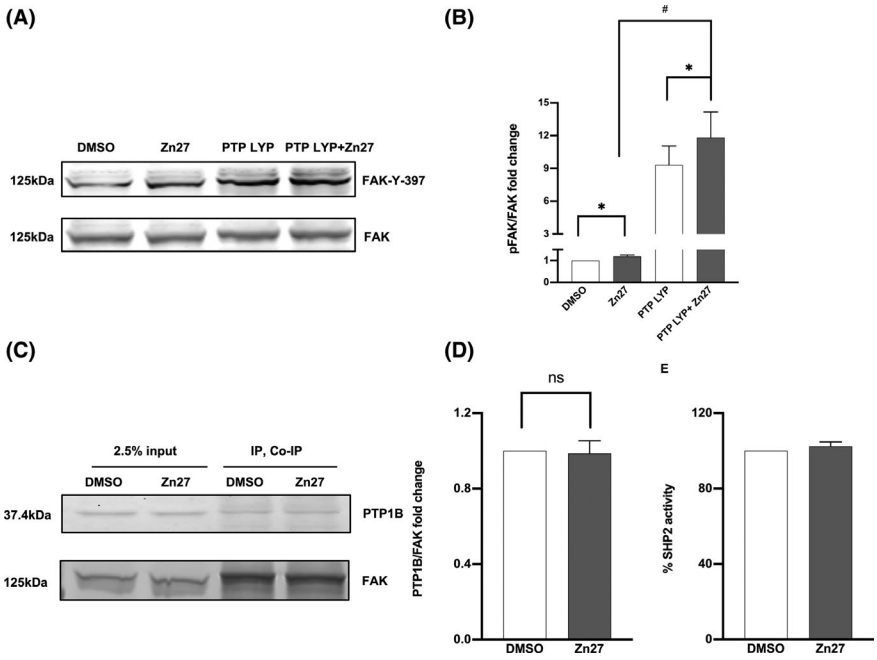

FIGURE 1 Studies of potential interactions between Zn27 and the tyrosine phosphatases that inactivate FAK. (A) Zn27 (10 nM) stimulated FAK-Tyr-397 phosphorylation as measured by Western blot in Caco-2 cells without or with PTP LYP inhibitor (50 μM) ($n = 25$, $^*p < .05$). (B) Densitometric analysis of the blots described in (A) Because PTP LYP inhibition dramatically accentuated FAK phosphorylation, a Y-axis break has been placed to be able to visually represent the effects of Zn27 on FAK phosphorylation in both the absence and presence of PTP LYP inhibitor on the same graph. (C) Lack of effect of 10 nM Zn27 on FAK-PTP1B association in suspended Caco-2 cells. Cell lysates were immunoprecipitated with anti-FAK and then blotted for either co-precipitating PTP1B (top panel) or FAK itself (bottom panel). Input is shown in the first two lanes and the immunoprecipitant in the third and fourth lanes. (D) Densitometric analysis of eight similar studies to the one shown in C demonstrates that treating with Zn27 (10 nM) does not affect the amount of PTP1B co-precipitating with FAK ($n = 8$) (E) Lack of effect of Zn27 (100 nM) on SHP2 activity ($n = 2$). All data are represented as mean ± SE, $^*p < .05$

His-tagged FAK kinase domain (35 kDa), each synthesized from baculovirus (Figure 2C). Using a cell-free system, the purified form for full-length FAK (125 kDa) and FAK kinase domain (35 kDa) was incubated for 30 min in the presence of ATP without and with 10 nM Zn27, resolved by SDS-PAGE, and then blotted with an antibody that recognizes the Tyr-397 phosphorylated form of FAK. Zn27 significantly stimulated FAK-Tyr-397 autophosphorylation of both the full-length FAK (125 kDa) (1.12 ± 0.02, $n = 9$, $p < .05$) and the kinase (35 kDa) domain of FAK (1.22 ± 0.1, $n = 8$, $p < .05$) outside cells and in the absence of other signaling molecules (Figure 2D).

Because these results suggested that Zn27 interacts with FAK directly, we next evaluated the effects of Zn27 on the kinase activity of full-length FAK and its kinase domain. Using a luminescent ADP detection system, we observed a significantly increased kinase activity for both full-length FAK (1.25 ± 0.07, $n = 4$, $p < .05$) and its kinase domain (1.14 ± 0.05, $n = 4$, $p < .05$) compared to control (Figure 2E and F). However, we observed no increase in kinase activity when 10 nM Zn21, a structural isomer of Zn27, was combined with the FAK kinase domain in this same system, suggesting the selectivity of the observation (Figure 2F). Finally, to determine the optimal activating concentration of Zn27 in vitro, we used this same luminescent ADP detection system with the purified FAK kinase domain over a range of Zn27 concentrations. Zn27 dose-dependently stimulated kinase activity with a calculated EC_{50} of 0.3 ± 1.7 nM ($n = 9$). These results suggest that Zn27 is a direct and highly potent activator of FAK (Figure 2G). Analysis of dose–response data was performed using nonlinear regression which allows for a variable slope. The slope for Zn27 dose–response curve for the FAK kinase domain was shallow with a Hill coefficient of 0.53 ± 0.18.

3.3 | Zn27 competes with the inhibitor PF573228 to activate FAK

The kinase inhibitor PF573228 competitively interacts at the ATP-binding pocket of FAK to prevent FAK-Tyr-397

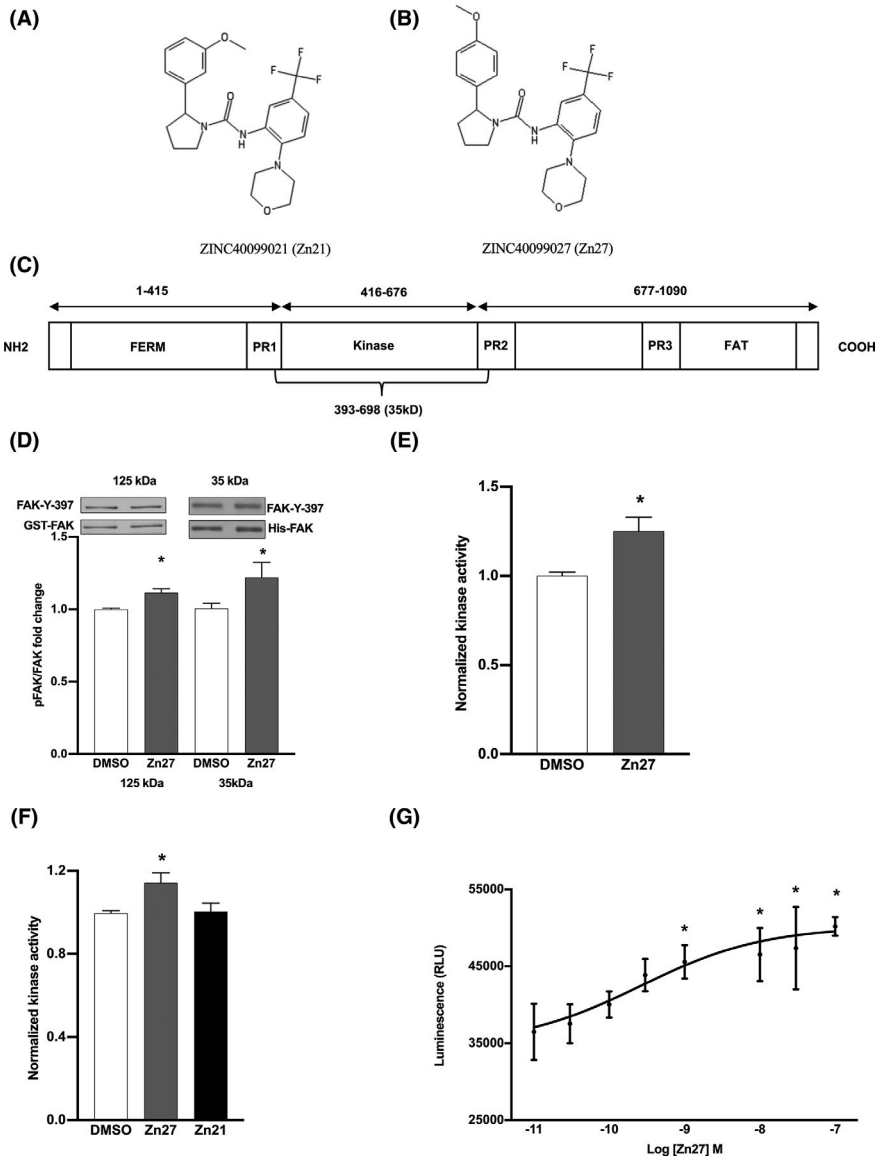

FIGURE 2 Zn27 directly stimulates the activity of FAK. The chemical structures (A) ZINC40099021 (Zn21) and (B) ZINC40099027 (Zn27) drawn using PubChem Sketcher (https://pubchem.ncbi.nlm.nih.gov//edit3/index.html).[84] (C) A schematic diagram represents the different domains of FAK. (D) Zn27 (10 nM) directly stimulates the Tyr-397 autophosphorylation of full length (125 kDa) (Figure represents pooled data from 9 experiments with 4 replicates in each experiment, $n = 9$, $^*p < .05$) and 35 kDa FAK (Figure represents pooled data from 8 experiments with 4 replicates in each experiment, $n = 8$, $^*p < .05$). (E) Zn27 stimulates the conversion of ATP to ADP by highly purified full-length 125 kDa human FAK in an in vitro kinase assay (Figure represents pooled data from 3 experiments with 5 replicates in each experiment, $n = 3$, $^*p < .05$) (F) Zn27 binding stimulates the conversion of ATP to ADP by the 35 kDa FAK kinase domain in an in vitro kinase assay compared to negative control Zn21 (Figure represents pooled data from 2 experiments with 4 replicates in each experiment, $n = 2$, $^*p < .05$). (G) Dose–response curve of Zn27 as an agonist of the 35 kDa kinase domain of FAK. (Figure represents pooled data from 9 experiments with 3 replicates in each experiment, $n = 9$, $^*p < .05$)

auto-phosphorylation.[35] We used PF573228 as a pharmacological tool to further substantiate the direct interaction of Zn27 with FAK. We explored the effects of combining Zn27 and PF573228 on FAK activity in intact Caco-2 cells. When Caco-2 cells were stimulated with 10 nM Zn27 for an hour, Western blots with anti-Tyr-397-FAK antibody demonstrated a significant increase in the phosphorylation (active) state of FAK (1.22 ± 0.07 fold over basal, $n = 8$, $p < .05$). However, when Caco-2 cells were incubated with both PF573228 and Zn27, Zn27 was still able to stimulate FAK phosphorylation even in the presence of PF573228 to 148.7 ± 3.35% of FAK phosphorylation in the presence of the inhibitor alone. ($n = 8$, $p < .05$, Figure 3A). These results further clarify the direct effect Zn27 has on FAK activity and the competitive nature of this interaction.

We further explored the interaction of Zn27 and PF573228 in the purified in vitro kinase system. Using the cell-free luminescent ADP detection system to measure 35 kDa FAK kinase domain activity, we studied increasing amounts of PF573228 in the presence or absence of 10 nM Zn27 to calculate effective inhibitory concentrations. PF573228 was able to completely inhibit FAK activity in a concentration-dependent manner in both the absence and presence of Zn27 (Figure 3B). The IC_{50} for PF573228 to inhibit FAK activity was essentially the same, calculated to be 8.4 ± 0.04 nM and 9.0 ± 0.03 nM, with and without Zn27, respectfully.

To assess the potential competitive properties of Zn27, we again used the cell-free luminescent ADP detection system to measure 35 kDa FAK activity with increasing concentrations of Zn27 in the absence or presence of a single effective concentration of PF573228 (Figure 3C). We observed a statistically significant difference for the kinase activity at each Zn27 concentration (0.01, 0.1, 1, 10, 100 nM) in the presence or absence of PF573228 (Figure 3C, $n = 21$, $^*p < .05$, representing statistical difference in kinase activity between Zn27 alone and Zn27+PF573228 at each Zn27 concentration). The concentration–response curve for Zn27 alone suggested a concentration-dependent increase in kinase activity with an EC_{50} of 0.28 ± 0.07 nM. However, in the presence of 10 nM PF573228 the concentration–response curve was right-shifted. Indeed, we

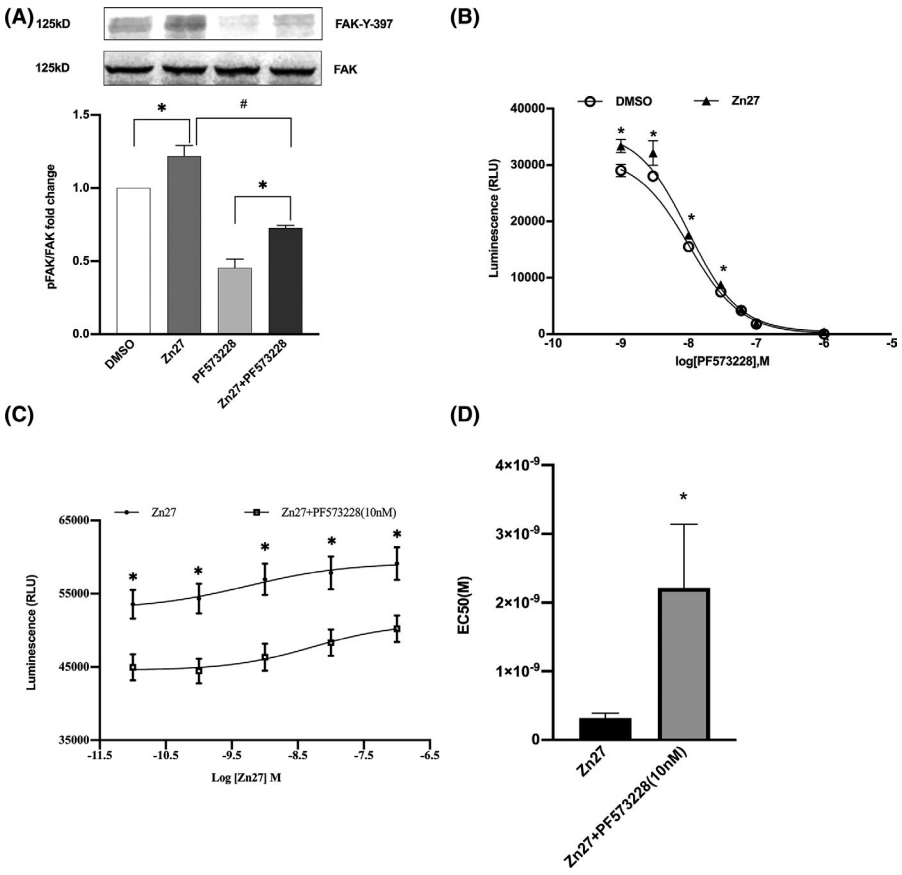

FIGURE 3 Competition displacement study (A) The effect of PF573228 (10 μM) on Zn27 (10 nM) induced phosphorylation of FAK-Tyr-397 in suspended Caco-2 cells ($p < .05$, $n = 8$, * Zn27 significant vs. DMSO $p < .05$; * Zn27+PF573228 (10, 100, 1000 nM) significant vs. DMSO, $p < .05$; # Zn27+PF573228 significant vs. Zn27 $p < .05$). (B) Dose-dependent inhibition of Zn27 (10 nM) activation of 35 kDa FAK kinase domain by PF573228 (IC50 8.4 ± 0.04 nM). (Figure represents pooled data from 9 experiments with 4 replicates in each experiment, $n = 9$, $^*p < .05$). (C) Concentration-dependent activation of 35 kDa kinase domain of FAK by Zn27 in the absence or presence of PF573228 (10 nM). *'s represents comparison of luminescence at varying concentrations of Zn27 in the absence or presence of 10 nM PF573228. Increasing concentration of Zn27 causes a rightward shift of the concentration–response curve. Figure represents pooled data from 21 experiments with 3 replicates in each experiment, $n = 21$, $^*p < .05$. (D) EC_{50} for Zn27 in absence and presence of 10 nM PF573228 ($n = 21$, $^*p < .05$)

calculated a statistically significant eight-fold increase in the EC_{50} in the presence of 10 nM PF573228 to 2.2 ± 0.9 nM (Figure 3D, $n = 21$, $p < .05$). Together, these results suggest a competitive property of Zn27 for stimulating FAK activity in a cell-free system.

3.4 | Characterization of Zn27-FAK activation kinetics

Since Zn27 directly interacts with the purified kinase domain of FAK to potently increase activity, we investigated the characteristics of this interaction using a saturation enzyme kinetics assay to calculate any changes in Michaelis–Menten kinetic parameters caused by Zn27. The luminescent ADP detection system was used with increasing concentrations of ATP (0–300 μM) and 12.5 ng or 357 nM of purified FAK kinase domain in the absence and presence of 10 nM Zn27 to generate total and nonspecific plots (Figure 4A and B). Specific activity was calculated by subtracting nonspecific from the total activity for each data point. Specific activity was then best fitted to the Michaelis–Menten equation using nonlinear regression analysis to calculate the apparent K_m and V_{max}. There were important and significant differences calculated for specific saturation kinetics parameters in the presence of Zn27 when compared with control (Figure 4C). For instance, the maximum FAK kinase velocity (V_{max}) in the presence of Zn27 was significantly greater (273 ± 27 μmol/min/ng, $n = 5$, $p < .05$) when compared with that calculated for control (208 ± 27 μmol/min/ng kinase, Figure 4D). Additionally, the apparent K_m of ATP for FAK calculated in the presence of Zn27 was significantly higher (12.6 ± 1.0 μM, $n = 5$, $p < .05$) when compared with the apparent K_m of ATP for FAK calculated control (6.4 ± 1.2 μM, Figure 4E).

4 | DISCUSSION

In this study, we characterize the pharmacological properties and molecular mechanism of a small molecule specific activator of FAK, Zn27. FAK has been well studied as a regulator of growth signaling, cell proliferation, adhesion, and epithelial sheet migration and mucosal healing.[6,19,24,36–38] This study was prompted by the observation that Zn27 promotes mucosal wound healing by activating FAK via phosphorylation of Tyr-397 and that Zn27 does not activate either the most closely related kinase, Pyk2, or another paradigmatic nonreceptor tyrosine kinase, Src.[21] This study shows that Zn27 does not modulate FAK indirectly by modulating tyrosine phosphatase activity but rather interacts directly with the kinase domain of FAK itself. Furthermore, because Zn27 in a concentration-dependent manner surmounted the effect of the ATP-competitive inhibitor for FAK, PF573228, Zn27 may act as an allosteric FAK activator to overcome the inhibitor's influence on the kinase.

Zn27 was originally chosen because of its structural similarity to residues 113–117 (Leu-Ala-His-Pro-Pro) of the FERM domain of FAK.[20] Zn27 follows "Lipinski's rule of five" with a molecular weight of 449.5, a single hydrogen bond donor, four hydrogen bond acceptors, five rotational hydrogens, and a partition coefficient of 3.726.[39] This makes Zn27 a useful jumping-off point for drug discovery. Having noted that Zn27 activates FAK in suspended colon cancer cells,[20] we extended this work to demonstrate activation of FAK in

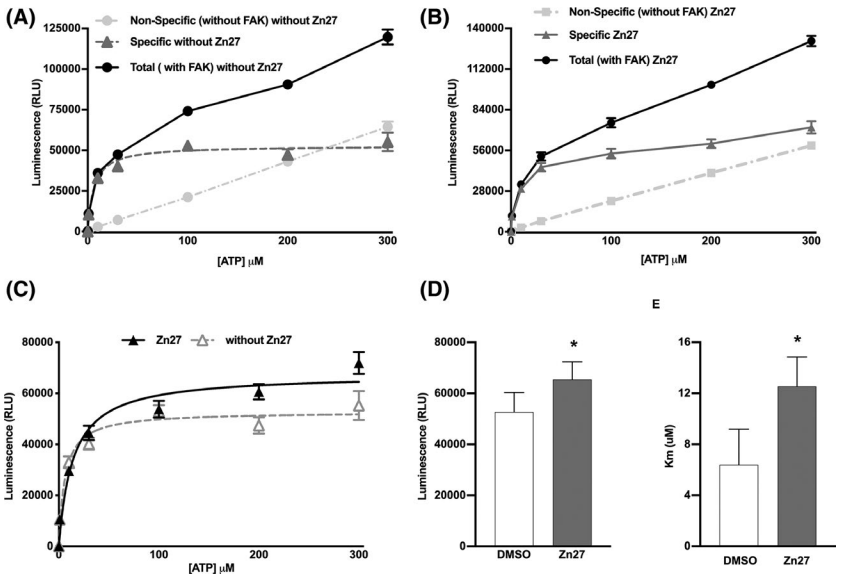

FIGURE 4 Saturation-binding assay for ATP in the presence or absence of FAK for Zn27 (10 nM). The saturation curve representing the total binding, specific binding, and nonspecific-binding activity of FAK with increasing concentrations (0–300 μM) of ATP (A) DMSO (B) Zn27 (10 nM). (Figure represents pooled data from 6 experiments with 3 replicates in each experiment, $n = 6$, $^*p < .05$) (C) Specific binding for ATP was determined in the presence or absence of Zn27 (10 nM). Specific binding = Total-(Nonspecific) (Figure represents pooled data from 6 experiments with 3 replicates in each experiment, $n = 6$, $^*p < .05$) (D and E) Effect of Zn27 (10 nM) on V_{max} (D) and K_m (E). The figure represents pooled data from six experiments with three replicates in each experiment, $n = 6$, $^*p < .05$

human Caco-2 epithelial cells,[21] which are a common model for intestinal biology,[15,37,40] as well as in the intestinal mucosa at the edge of healing wounds in mice.[21] Zn27 seems selective to FAK as it does not activate the tyrosine kinase most closely related to FAK (Pyk-2) or another prototypical nonreceptor tyrosine kinase also located in the focal adhesion complex (c-Src).[21]

If Zn27 activates FAK in cells, it remains to be established how this happens. FAK activation begins with its autophosphorylation at tyrosine 397.[41] Protein phosphorylation represents a balance between kinases and phosphatases.[42] Indeed, phosphatases that dephosphorylate FAK promote cell migration and adhesion.[43,44] It, therefore, seemed an attractive hypothesis that Zn27 might interact with one of the classical tyrosine-specific nonreceptor protein phosphatases (SHP2, PTP1B, PTP-PEST) that have been identified as key players in modulating both FAK activity[45–47] and cell migration.[48] Although PTP-PEST modulates FAK-Tyr-397 dephosphorylation,[44] FAK activity,[46,49] and cell migration,[50,51] PTP-PEST inhibition, accentuated basal FAK phosphorylation, but did not prevent Zn27 further stimulation of FAK Tyr-397. Similarly, although the tyrosine phosphatase PTP1B also dephosphorylates FAK,[52] we did not observe any change in PTP1B/FAK activity with Zn27. Finally, SHP2 is the third of the key phosphatases known to dephosphorylate and inactivate FAK and promote cell migration.[47,53] However, Zn27 did not alter SHP2 activity. These results were thus not consistent with the hypothesis that Zn27 activates FAK by inhibiting relevant tyrosine phosphatases.

We, therefore, turned our attention to the possibility that Zn27 interacts directly with FAK. Zn27 in our current study activated FAK both within intact cells and in vitro in the absence of other cell signaling proteins. The calculated EC_{50} for Zn27, in cell-free system was 0.3 ± 1.7 nM. That is, Zn27 at 0.3 ± 1.7 nM yielded half the maximal effect. EC50 is commonly considered a measure of potency, and an EC50 in the nanomolar range would thus be considered potentially potent.[54] Although the effect of this molecule on FAK activation itself might seem relatively modest, FAK sits atop an increasingly amplifying signal cascade, so downstream signals might be more vigorous. In a previous study, we demonstrated that intraperitoneal injection of Zn27 at 900ug/kg resulted in peak levels of approximately 22.25 nM at 1 h and trough levels of approximately 4.6 nM by 6 h. Four days after the creation of an ischemic mucosal jejunal ulcer and 3 days after the commencement of treatment 1 day later, we observed the trough levels fell slightly below the threshold that seemed required for in vitro efficacy. Despite this, we observed increased activation of FAK in the epithelium at the edge of mucosal ulcers and found that healing was accelerated approximately fourfold compared that observed in ulcers in vehicle-treated control mice.[21] In a patient with a bleeding GI ulcer, for instance, such an acceleration might well make the difference between successful conservative treatment and the need for surgery. In the future, modifications of the molecule itself to make it more potent or modifications of the dosing or drug delivery schedule might further increase the in vivo effect.

The Hill coefficient or interaction coefficient is an important measure for dose–response related to cooperativity for multiple binding site.[55] A Hill coefficient greater than 1 suggests positive cooperativity with steep slopes whereas a Hill coefficient less than 1 suggests negative cooperativity by shallow slopes,[56] meaning that binding of one ligand to the receptor makes it much more difficult for subsequent ligand to bind.[57] Hence, the shallow slope we observed here suggests that if one Zn27 molecule binds to the FAK kinase domain then binding of another Zn27 to the domain is more difficult. However, previous studies have studied drugs with shallow slopes.[56,58–60]

Such apparent negative cooperativity could be explained in at least two ways. Either more than one Zn27 molecule can bind to the FAK kinase domain, further activating it or there is dimerization of the FAK kinase domain such that Zn27 could bind to each unit of a FAK dimer. Although full-length FAK does dimerize and indeed this may be important for its further activation, such dimerization seems to occur by FERM: FERM, FAT: FERM, and FAT: FAT domain interactions, whereas FAK kinase domain dimerization has not been reported.[61,62] This, therefore, raises the possibility that Zn27 may effectively bind to more than one site on the FAK kinase domain, and that this multiple binding evidence negative cooperativity. The activation of full-length FAK in situ is considerably more complex than activation of the kinase domain alone, involving unmasking of the kinase domain by the N-terminal FERM domain,[63] further modulation dependent on the dimerization of full-length FAK,[61,62] and interaction with other kinases such as Src [64] and other molecules.[65] Thus, it remains to be explored whether the negative cooperativity we observed here with the purified kinase domain is important in intact cells. Indeed, despite the negative cooperativity that Zn27 appears to exhibit with the purified kinase domain in solution, Zn27 appears effective both in cells and in mice.[21] Future studies may further explore structure–activity relationships for this molecule and attempt to modify its cooperativity for receptor–ligand interaction.

Our further analysis demonstrated that Zn27 interacts selectively with the 35 kD FAK kinase domain. FAK includes a FERM domain (1–420aa), a kinase domain (421–680aa), and a C terminal focal adhesion targeting (FAT) domain (840–1052aa; 66; Figure 2A). The FAT domain targets focal adhesion sites, whereas the FERM domain is an autoinhibitory site for the kinase domain, regulating FAK catalytic activity.[67] Tyr-397 is a key autophosphorylation site for FAK activity [68] and the release of the FERM domain from the kinase domain leads to FAK autophosphorylation, increasing kinase activity.[69–71] Since Zn27 was originally designed for similarities in conformation to a small critical subdomain of the FERM domain,[20] it, therefore, seems attractive to further hypothesize that Zn27 somehow competes with the FERM domain for binding to the kinase domain, preventing full blockade of the kinase domain by the FERM domain and thereby facilitating FAK activation. However, this possibility awaits further study.

PF573228 is an ATP-competitive inhibitor of FAK, inhibiting Tyr-397 phosphorylation with an IC_{50} of 4 nM in a cell-free

assay.[35,72,73] As both PF573228 and Zn27 are acting to modulate FAK-Tyr-397 phosphorylation, we used competition studies with PF573228 to investigate the properties of Zn27. Our studies using increasing concentrations of Zn27 in the presence of an effective PF573228 concentration showed the classical properties of orthosteric ligands competitively interacting with each other. The shift of curve to right in presence of antagonist is an example of functional antagonism with a similar target of drug[74] action (,[75] For varying concentrations of agonist, the basal activity is decreased for a specific concentration of antagonist.[75] In our study, the basal activity for Zn27 was completely antagonized in presence of PF573228 with a shift in the curve to the right, and the EC50 was lowered, indicating a type of functional antagonism with a similar target for drug action. However, when conditions were reversed, there were no differences in the PF573228 IC_{50} even in the presence of Zn27 when compared with control. These results indicate to us that Zn27 is interacting with the kinase domain of FAK at a site allosteric from where ATP or PF573228 binds. How Zn27 specifically interacts with the FAK kinase domain awaits further exploration.

The kinetics of Zn27 activation of FAK shows that Zn27 increases both the FAK K_m and V_{max}. An increase in maximal kinase activity at saturating ATP concentrations (V_{max}) is not an unexpected activating property for Zn27. We also observed an increase in the ATP concentration needed to achieve half-maximal FAK activity (K_m). Previous studies have estimated in vivo intracellular ATP to be in the range of 0.01–0.1 mM,[76] whereas ATP concentrations that saturate in vitro kinase assays are in the micromolar range.[77–80] Thus, within cells, FAK is likely to already be exposed to an excess of ATP, and the increased K_m in the presence of Zn27 is likely not detrimental to kinase activity. Others have also described activators that increase both the K_m and V_{max} of a reaction.[81–83] Of interest is that these authors describe the interactions of such activators with the enzyme as allosteric from the substrate-binding site.

In summary, Zn27 is a promising molecule that follows Lipinski's rule and has many drug-like properties. This study demonstrates that Zn27 interacts directly with the kinase domain of FAK to stimulate FAK activity. Previous work suggests that the increased FAK activation promotes epithelial monolayer wound closure in vitro and intestinal epithelial mucosal wound healing in mouse models.[21] Taken together with this previous study, these results describe Zn27 as a novel, potent, and selective activator acting on 35 kDa FAK kinase domain and suggest the selective interaction to be allosteric for the kinase domain of FAK.

ACKNOWLEDGMENTS

The research reported in this publication was supported by the National Institute of General Medicine of the National Institutes of Health under award number UT2GM130175.

CONFLICTS OF INTEREST

The authors declare no conflict of interest.

AUTHOR CONTRIBUTIONS

Rashmi, Shyam K More, Qinggang Wang, Emilie E. Vomhof-DeKrey, James E. Porter, and Marc D. Basson participated in research design and wrote or contributed to the writing of the manuscript. Rashmi, Shyam K More, and Qinggang Wang conducted the experiments and performed data analysis. James E. Porter and Marc D. Basson also participated in data analysis.

ETHICAL STATEMENT

Hereby, I Rashmi consciously assure that for the manuscript "ZINC40099027 activates human Focal Adhesion Kinase by accelerating the enzymatic activity of the FAK kinase domain" the following is fulfilled:

1. This material is the authors' own original work, which has not been previously published elsewhere.
2. The paper is not currently being considered for publication elsewhere.
3. The paper reflects the authors' own research and analysis in a truthful and complete manner.
4. The paper properly credits the meaningful contributions of co-authors and co-researchers.
5. The results are appropriately placed in the context of prior and existing research.
6. All sources used are properly disclosed (correct citation). Literally copying of text must be indicated as such by using quotation marks and giving proper reference.
7. All authors have been personally and actively involved in substantial work leading to the paper and will take public responsibility for its content.

DATA AVAILABILITY STATEMENT

The data that support the findings of the study are available from the corresponding author upon reasonable request.

ORCID

Marc D. Basson https://orcid.org/0000-0001-9696-2789

REFERENCES

1. Froslie, KF, Jahnsen, J, Moum, BA, Vatn, MH; IBSEN Group. Mucosal healing in inflammatory bowel disease: results from a Norwegian population-based cohort. *Gastroenterology*. 2007;133:412-422.
2. Basson MD. Hierarchies of healing in gut mucosal injury. *J Physiol Pharmacol*. 2017;68(6):789-795.
3. Basson MD, Modlin IM, Madri JA. Human enterocyte (Caco-2) migration is modulated in vitro by extracellular matrix composition and epidermal growth factor. *J. Clin Investig*. 1992;90:15-23.
4. Nusrat A, Delp C, Madara JL. Intestinal epithelial restitution. Characterization of a cell culture model and mapping of cytoskeletal elements in migrating cells. *J Clin Investig*. 1992;89:1501-1511.
5. Guan QA. Comprehensive review and update on the pathogenesis of inflammatory bowel disease. *J Immunol Res*. 2019;2019:7247238.
6. Sanders MA, Basson MD. Collagen IV regulates Caco-2 migration and ERK activation via alpha1beta1- and alpha2beta1-integrin-dependent Src kinase activation. *Am J Physiol Gastrointest Liver Physiol*. 2004;286:G547-G557.

7. Alam A, Neish A. Role of gut microbiota in intestinal wound healing and barrier function. *Tissue Barriers*. 2018;6:1539595.
8. Yue B, Luo X, Yu Z, Mani S, Wang Z, Dou W. Inflammatory bowel disease: a potential result from the collusion between gut microbiota and mucosal immune system. *Microorganisms*. 2019;7:440.
9. Basson MD, Emenaker NJ, Hong F. Differential modulation of human (Caco-2) colon cancer cell line phenotype by short-chain fatty acids. *Proc Soc Exp Biol Med*. 1998;217:476-483.
10. Priyadarshini M, Kotlo KU, Dudeja PK, Layden BT. Role of short chain fatty acid receptors in intestinal physiology and pathophysiology. *Compr Physiol*. 2018;8:1091-1115.
11. Webb DJ, Donais K, Whitmore LA, et al. FAK-Src signaling through paxillin, ERK, and MLCK regulate adhesion disassembly. *Nat Cell Biol*. 2004;6:154-161.
12. Furuyama K, Doi R, Mori T, et al. Clinical significance of focal adhesion kinase in resectable pancreatic cancer. *World J Surg*. 2006;30:219-226.
13. Zhao X, Guan JL. Focal adhesion kinase and its signaling pathways in cell migration and angiogenesis. *Adv Drug Deliv Rev*. 2011;63:610-615.
14. Provenzano PP, Keely PJ. The role of focal adhesion kinase in tumor initiation and progression. *Cell Adh Migr*. 2009;3:347-350.
15. Chaturvedi LS, Gayer CP, Marsh HM, Basson MD. Repetitive deformation activates Src-independent FAK-dependent ERK motogenic signals in human Caco-2 intestinal epithelial cells. *Am J Physiol Cell Physiol*. 2008;294:C1350-C1361.
16. Chaturvedi LS, Marsh HM, Basson MD. Role of RhoA and its effectors ROCK and mDia1 in the modulation of deformation-induced FAK, ERK, p38, and MLC motogenic signals in human Caco-2 intestinal epithelial cells. *Am J Physiol Cell Physiol*. 2011;301:C1224-C1238.
17. Walsh MF, Thamilselvan V, Grotelueschen R, Farhana L, Basson M. Absence of adhesion triggers differential FAK and SAPKp38 signals in SW620 human colon cancer cells that may inhibit adhesiveness and lead to cell death. *Cell Physiol Biochem*. 2003;13:135-146.
18. Yu CF, Sanders MA, Basson MD. Human Caco-2 motility redistributes FAK and paxillin and activates p38 MAPK in a matrix-dependent manner. *Am J Physiol Gastrointest Liver Physiol*. 2000;278:G952-G966.
19. Walsh MF, Ampasala DR, Hatfield J, et al. Transforming growth factor-beta stimulates intestinal epithelial focal adhesion kinase synthesis via Smad- and p38-dependent mechanisms. *Am J Pathol*. 2008;173:385-399.
20. Raschka S, More SK, Devadoss D, Zeng B, Kuhn LA, Basson MD. Identification of potential small-molecule protein-protein inhibitors of cancer metastasis by 3D epitope-based computational screening. *J Physiol Pharmacol*. 2018;69(2):255-263.
21. Wang Q, More SK, Vomhof-DeKrey EE, Golovko MY, Basson MD. Small molecule FAK activator promotes human intestinal epithelial monolayer wound closure and mouse ulcer healing. *Sci Rep*. 2019;9:14669.
22. Lai IR, Chu PY, Lin HS, et al. Phosphorylation of focal adhesion kinase at Tyr397 in gastric carcinomas and its clinical significance. *Am J Pathol*. 2010;177:1629-1637.
23. Basson MD, Wang Q, Chaturvedi LS, et al. Schlafen 12 interaction with serpinB12 and deubiquitylases drives human enterocyte differentiation. *Cell Physiol Biochem*. 2018;48:1274-1290.
24. Conway WC, der Voort V, van Zyp J, et al. Paxillin modulates squamous cancer cell adhesion and is important in pressure-augmented adhesion. *J Cell Biochem*. 2006;98:1507-1516.
25. DeMoe JH, Santaguida S, Daum JR, Musacchio A, Gorbsky GJ. A high throughput, whole cell screen for small molecule inhibitors of the mitotic spindle checkpoint identifies OM137, a novel Aurora kinase inhibitor. *Cancer Res*. 2009;69:1509-1516.
26. Motulsky HJ, Ransnas LA. Fitting curves to data using nonlinear regression: a practical and nonmathematical review. *FASEB J*. 1987;1:365-374.
27. Jaccard J, Becker MA, Wood G. Pairwise multiple comparison procedures: a review. *Psychol Bull*. 1984;96:589-596.
28. Faul F, Erdfelder E, Lang A, Buchner A. G*Power 3: a flexible statistical power analysis program for the social, behavioral, and biomedical sciences. *Behav Res Methods*. 2007;39:175-191.
29. Harding SD, Sharman JL, Faccenda E, et al. The IUPHAR/BPS Guide to PHARMACOLOGY in 2019: updates and expansion to encompass the new guide to IMMUNOPHARMACOLOGY. *Nucleic Acids Res*. 2018;46:D1091-D1106. https://doi.org/10.1093/nar/gkx1121
30. Grinnell KL, Casserly B, Harrington EO. Role of protein tyrosine phosphatase SHP2 in barrier function of pulmonary endothelium. *Am J Physiol Lung Cell Mol Physiol*. 2010;298:L361-L370.
31. Faisal A, El-Shemerly M, Hess D, Nagamine Y. Serine/threonine phosphorylation of ShcA. Regulation of protein-tyrosine phosphatase-pest binding and involvement in insulin signaling. *J Biol Chem*. 2002;277:30144-30152.
32. Garton AJ, Tonks NK. PTP-PEST: a protein tyrosine phosphatase regulated by serine phosphorylation. *EMBO J*. 1994;13(16):3763-3771.
33. Feldhammer M, Uetani N, Miranda-Saavedra D, Tremblay ML. PTP1B: a simple enzyme for a complex world. *Crit Rev Biochem Mol Biol*. 2013;48:430-445.
34. Karver MR, Krishnamurthy D, Kulkarni RA, Bottini N, Barrios AM. Identifying potent, selective protein tyrosine phosphatase inhibitors from a library of Au(I) complexes. *J Med Chem*. 2009;52:6912-6918.
35. Slack-Davis JK, Martin KH, Tilghman RW, et al. Cellular characterization of a novel focal adhesion kinase inhibitor. *J Biol Chem*. 2007;282:14845-14852.
36. Hamidi H, Pietila M, Ivaska J. The complexity of integrins in cancer and new scopes for therapeutic targeting. *Br J Cancer*. 2016;115:1017-1023.
37. Owen KA, Abshire MY, Tilghman RW, Casanova JE, Bouton AH. FAK regulates intestinal epithelial cell survival and proliferation during mucosal wound healing. *PLoS One*. 2011;6:e23123.
38. Thamilselvan V, Basson MD. The role of the cytoskeleton in differentially regulating pressure-mediated effects on malignant colonocyte focal adhesion signaling and cell adhesion. *Carcinogenesis*. 2005;26:1687-1697.
39. Lipinski CA. Lead- and drug-like compounds: the rule-of-five revolution. *Drug Discov Today Technol*. 2004;1:341-337.
40. Basson MD, Sanders MA, Gomez R, et al. Focal adhesion kinase protein levels in gut epithelial motility. *Am J Physiol Gastrointest Liver Physiol*. 2006;291:G491-G499.
41. Heim JB, McDonald CA, Wyles SP, et al. FAK auto-phosphorylation site tyrosine 397 is required for development but dispensable for normal skin homeostasis. *PLoS One*. 2018;13:e0200558.
42. Stoker AW. Receptor tyrosine phosphatases in axon growth and guidance. *Curr Opin Neurobiol*. 2001;11:95-102.
43. Manes S, Mira E, Gomez-Mouton C, Zhao ZJ, Lacalle RA, Martínez-A C. Concerted activity of tyrosine phosphatase SHP2 and focal adhesion kinase in regulation of cell motility. *Mol Cell Biol*. 1999;19:3125-3135.
44. Zheng Y, Yang W, Xia Y, Hawke D, Liu DX, Lu Z. Ras-induced and extracellular signal-regulated kinase 1 and 2 phosphorylation-dependent isomerization of protein tyrosine phosphatase (PTP)-PEST by PIN1 promotes FAK dephosphorylation by PTP-PEST. *Mol Cell Biol*. 2011;31:4258-4269.
45. Chen Z, Morales JE, Guerrero PA, Sun H, McCarty JH. PTPN12/PTP-PEST regulates phosphorylation-dependent ubiquitination and stability of focal adhesion substrates in invasive glioblastoma cells. *Cancer Res*. 2018;78:3809-3822.
46. Gonzalez Wusener AE, González Á, Nakamura F, Arregui CO. PTP1B triggers integrin-mediated repression of myosin activity and modulates cell contractility. *Biol Open*. 2015;5:32-44.
47. Hartman ZR, Schaller MD, Agazie YM. The tyrosine phosphatase SHP2 regulates focal adhesion kinase to promote EGF-induced lamellipodia persistence and cell migration. *Mol Cancer Res*. 2013;11:651-664.

48. Larsen M, Tremblay M, Yamada K. Phosphatases in cell–matrix adhesion and migration. *Nat Rev Mol Cell Biol*. 2003;4:700-711.
49. Burdisso JE, González Á, Arregui CO. PTP1B promotes focal complex maturation, lamellar persistence and directional migration. *J Cell Sci*. 2013;126(Pt 8):1820-1831.
50. Angers-Loustau A, Côté JF, Charest A, et al. Protein tyrosine phosphatase-PEST regulates focal adhesion disassembly, migration, and cytokinesis in fibroblasts. *J Cell Biol*. 1999;144:1019-1031.
51. Zheng Y, Lu Z. Regulation of tumor cell migration by protein tyrosine phosphatase (PTP)-proline-, glutamate-, serine-, and threonine-rich sequence (PEST). *Chin J Cancer*. 2013;32:75-83.
52. Arregui CO, Gonzalez A, Burdisso JE, González Wusener AE. Protein tyrosine phosphatase PTP1B in cell adhesion and migration. *Cell Adh Migr*. 2013;7:418-423.
53. Yu DH, Qu CK, Henegariu O, Lu X, Feng GS. Protein-tyrosine phosphatase SHP2 regulates cell spreading, migration, and focal adhesion. *J Biol Chem*. 1998;273:21125-21131.
54. Gu J, Zhang X, Ma Y, et al. Quantitative modeling of dose-response and drug combination based on pathway network. *J Cheminform*. 2015;7:19.
55. Jenkins JL. Drug discovery: rethinking cellular drug response. *Nat Chem Biol*. 2013;9:669-670.
56. Weiss JN. The Hill equation revisited: uses and misuses. *FASEB J*. 1997;11:835-841.
57. Ha SH, Ferrell JE Jr. Thresholds and ultrasensitivity from negative cooperativity. *Science*. 2016;352:990-993.
58. Fallahi-Sichani M, Honarnejad S, Heiser LM, Gray JW, Sorger PK. Metrics other than potency reveal systematic variation in responses to cancer drugs. *Nat Chem Biol*. 2013;9:708-714.
59. Hsiao CC, Wiemer AJ. A power law function describes the time- and dose-dependency of Vγ9Vδ2 T cell activation by phosphoantigens. *Biochem Pharmacol*. 2018;158:298-304.
60. Shippy RR, Lin X, Agabiti SS, et al. Phosphinophosphonates and their tris-pivaloyloxymethyl prodrugs reveal a negatively cooperative butyrophilin activation mechanism. *J Med Chem*. 2017;60:2373-2382.
61. Brami-Cherrier K, Gervasi N, Arsenieva D, et al. FAK dimerization controls its kinase-dependent functions at focal adhesions. *EMBO J*. 2014;33:356-370.
62. Kleinschmidt EG, Schlaepfer DD. Focal adhesion kinase signaling in unexpected places. *Curr Opin Cell Biol*. 2017;45:24-30.
63. Cooper LA, Shen TL, Guan JL. Regulation of focal adhesion kinase by its amino-terminal domain through an autoinhibitory interaction. *Mol Cell Biol*. 2003;23:8030-8041.
64. Lietha D, Cai X, Ceccarelli DF, Li Y, Schaller MD, Eck MJ. Structural basis for the autoinhibition of focal adhesion kinase. *Cell*. 2007;129:1177-1187.
65. Frame MC, Patel H, Serrels B, Lietha D, Eck MJ. The FERM domain: organizing the structure and function of FAK. *Nat Rev Mol Cell Biol*. 2010;11:802-814.
66. Ceccarelli DF, Song HK, Poy F, Schaller MD, Eck MJ. Crystal structure of the FERM domain of focal adhesion kinase. *J Biol Chem*. 2006;281:252-259.
67. Zhou J, Bronowska A, Le Coq J, Lietha D, Gräter F. Allosteric regulation of focal adhesion kinase by PIP_2 and ATP. *Biophys J*. 2015;108:698-705.
68. Cobb BS, Schaller MD, Leu TH, Parsons JT. Stable association of pp60src and pp59fyn with the focal adhesion-associated protein tyrosine kinase, pp125FAK. *Mol Cell Biol*. 1994;14:147-155.
69. Chen SY, Chen HC. Direct interaction of focal adhesion kinase (FAK) with Met is required for FAK to promote hepatocyte growth factor-induced cell invasion. *Mol Cell Biol*. 2006;26:5155-5167.
70. Dunty JM, Gabarra-Niecko V, King ML, Ceccarelli DF, Eck MJ, Schaller MD. FERM domain interaction promotes FAK signaling. *Mol Cell Biol*. 2004;24:5353-5368.
71. Wang S, Basson MD. Akt directly regulates focal adhesion kinase through association and serine phosphorylation: implication for pressure-induced colon cancer metastasis. *Am J Physiol Cell Physiol*. 2011;300:C657-C670.
72. Fan H, Guan JL. Compensatory function of Pyk2 protein in the promotion of focal adhesion kinase (FAK)-null mammary cancer stem cell tumorigenicity and metastatic activity. *J Biol Chem*. 2011;286:18573-18582.
73. Zhang J, Fan G, Zhao H, et al. Targeted inhibition of focal adhesion kinase attenuates cardiac fibrosis and preserves heart function in adverse cardiac remodeling. *Sci Rep*. 2017;7:43146.
74. Avram G, Lewis A, Kalman Sumner M. Principles of drug action. The basis of pharmacology. *J Med Chem*. 1970;13:337.
75. Dhein S. Recording and analysing concentration-response curves. In: Dhein S, Mohr FW, Delmar M, eds. *Practical Methods in Cardiovascular Research*. Heidelberg: Springer, Berlin; 2005.
76. Huang H, Zhang X, Li S, et al. Physiological levels of ATP negatively regulate proteasome function. *Cell Res*. 2010;20:1372-1385.
77. Imamura H, Nhat KP, Togawa H, et al. Visualization of ATP levels inside single living cells with fluorescence resonance energy transfer-based genetically encoded indicators. *Proc Natl Acad Sci USA*. 2009;106:15651-15656.
78. Kennedy HJ, Pouli AE, Ainscow EK, Jouaville LS, Rizzuto R, Rutter GA. Glucose generates sub-plasma membrane ATP microdomains in single islet beta-cells. Potential role for strategically located mitochondria. *J Biol Chem*. 1999;274:13281-13291.
79. Sippel CJ, Dawson PA, Shen T, Perlmutter DH. Reconstitution of bile acid transportin a heterologous cell by cotransfection of transporters for bile acid uptake and efflux. *J Biol Chem*. 1997;272:18290-18297.
80. Wang RH, Tao L, Trumbore MW, Berger SL. Turnover of the acyl phosphates of human and murine prothymosin alpha in vivo. *J Biol Chem*. 1997;272:26405-26412.
81. Andersson D, Chakrabarty R, Bejai S, Zhang J, Rask L, Meijer J. Myrosinases from root and leaves of Arabidopsis thaliana have different catalytic properties. *Phytochemistry*. 2009;70:1345-1354.
82. Li X, Kushad MM. Purification and characterization of myrosinase from horseradish (*Armoracia rusticana*) roots. *Plant Physiol Biochem*. 2005;43:503-511.
83. Shikita M, Fahey JW, Golden TR, Holtzclaw WD, Talalay P. An unusual case of 'uncompetitive activation' by ascorbic acid: purification and kinetic properties of a myrosinase from Raphanus sativus seedlings. *Biochem J*. 1999;341(Pt 3):725-732.
84. Ihlenfeldt WD, Bolton EE, Bryant SH. The PubChem chemical structure sketcher. *J Cheminform*. 2009;1:20.

How to cite this article: Rashmi , More SK, Wang Q, Vomhof-DeKrey EE, Porter JE, Basson MD. ZINC40099027 activates human focal adhesion kinase by accelerating the enzymatic activity of the FAK kinase domain. *Pharmacol Res Perspect*. 2021;9:e00737. https://doi.org/10.1002/prp2.737